scientific reports

Check for updates

OPEN

Leishmania amazonensis impairs phagosome acidification in B-1 phagocytes as an unrecognized parasite infection and proliferation mechanism

Natalia S. Ferreira[1], Thalita C. S. Ferreira[1], Ismael P. Sauter[1], Deborah Brandt-Almeida[1], Daniela I. Staquicini[2,3], Josiane B. de Assis[4], Vivian C. de Oliveira[5], José Wandilson Barboza Duarte Júnior[5], Carla Claser[5], Ana Flavia Popi[5], Renata Pasqualini[2,3], Wadih Arap[2,6]✉ & Mauro Cortez[1,7]✉

Leishmaniasis is a neglected disease affecting people from tropical and subtropical areas. It is caused by protozoan parasites called *Leishmania* and transmitted by sandflies during blood meal. In phagocytic cells such as macrophages, *L. amazonensis* modulates endosomal/lysosomal trafficking pathways to form large parasitophorous vacuoles (PV) enabling parasite survival and proliferation. In this work, we report that upon invasion in a subset of phagocytic B (termed B-1P) cells, *L. amazonensis* survives and proliferates at high rates inside abnormally large and non-acid PV. Mechanistically, we show that the biogenesis of enlarged non-acidic lysosomal compartment is not directly linked to the regulation of the *LYST/Beige* gene that controls the expansion of *Leishmania*-PV in macrophages, but to the fusion of intracellular vesicles lacking V-ATPase, a proton pump required for the acidification. Finally, we show that B-1P cells host parasites that proliferate inside large non-acidic vacuoles at infection sites in immunocompetent mice. Thus, these pathophysiological alterations favor parasitic proliferation under in vitro and ex vivo conditions and reveal a heretofore unrecognized but key mechanistic role for B-1P cells in the progression of leishmaniasis. This study provides new experimental insights into a novel parasite evasion mechanism that might impact the host response during human disease development.

Keywords B-1 phagocytes, *Leishmania amazonensis*, *LYST/Beige* gene, Parasitophorous vacuole, V-ATPase

Leishmaniasis is a complex set of diseases caused by protozoan parasites of the genus *Leishmania*, transmitted to humans through the bite of infected female sandflies[1]. *Leishmania amazonensis* is among the most common species associated with patients presenting either with localized cutaneous leishmaniasis or with diffuse cutaneous leishmaniasis (DCL), a rare yet severe form of the disease[2].

The biology of *Leishmania* infection has been broadly defined in macrophages. In vivo, during the insect blood meal, infective promastigotes released from the digestive apparatus of the sandflies are engulfed by the host resident macrophages at the site of the insect bite; after phagocytosis, engulfed parasites transform into replicative amastigotes, which survive and multiply inside vacuolar structures termed parasitophorous vacuoles (PV)[3]. PV are highly acidic compartments containing multiple lytic enzymes including hydrolases, cathepsins, and ATP-dependent proton pumps (e.g., V-ATPases)[4,5] formed by the fusion of trafficking endosomes with

[1]Department of Parasitology, Institute of Biomedical Sciences, University of São Paulo, São Paulo, SP 05508, Brazil. [2]Rutgers Cancer Institute, Newark, NJ 07101, USA. [3]Division of Cancer Biology, Department of Radiation Oncology, Rutgers New Jersey Medical School, Newark, NJ 07103, USA. [4]Department of Immunology, Institute of Biomedical Sciences, University of São Paulo, São Paulo, SP 05508, Brazil. [5]Department of Microbiology, Immunology and Parasitology, Federal University of São Paulo, São Paulo, SP 04023, Brazil. [6]Division of Hematology/Oncology, Department of Medicine, Rutgers New Jersey Medical School, Newark, NJ 07103, USA. [7]Escuela de Tecnología Médica, Facultad de Ciencias, Pontificia Universidad Católica de Valparaíso, 2373223 Valparaíso, Chile. ✉email: wadih.arap@rutgers.edu; mcortez@usp.br

lysosomes, and by extensions of the endoplasmic reticulum[6]. Throughout evolution, in order to subvert such untoward conditions, *Leishmania* parasites have developed several mechanisms that enable survival and proliferation inside these PV. A classic example is described by parasites of *Leishmania mexicana* complex (*L. amazonensis*, *L. mexicana*, *L. pifanoi*, *L. venezuelensis*) that form large PV to attenuate the deleterious effect of inducible nitric oxide synthase and nitric oxide (iNOS/NO) in parasite multiplication[7]. As a countermeasure, host cells respond to parasite invasion by modulating multiple intracellular pathways to control parasite growth. For instance, macrophages infected with *L. amazonensis* up-regulate the transcription of the *LYST/Beige* gene, which encodes the lysosomal trafficking regulator LYST protein, to contain PV formation that restricts parasite growth[7,8]. Recently, our groups have described another host-parasite molecular mechanism that modulates the immune response by inducing the expression of CD200, an immune checkpoint inhibitor that restricts macrophage activation in vitro and reduces parasite load in vivo[9–11].

Although macrophages are generally considered the primary host cells, other cells—such as dendritic cells and/or lymphocytes—can be targeted by *Leishmania* infection[12]. B-cells have recently gained attention in studies of human DCL due to their elevated levels in skin lesions, which have been postulated to regulate macrophage phenotype to become permissive to parasite proliferation[13]. Despite this empirical finding, the full contribution of B-cells to the establishment and/or progression of leishmaniasis remains unclear. B-1 cells in particular, which are found mainly in the peritoneal and pleural cavities[14,15], comprise an ancient subset of B-cells featuring high expression of natural antibodies (IgM), co-expression of lymphoid and myeloid markers (e.g., CD19 and CD11b), along with the production of large amounts of interleukin (IL)−10[16]. The importance of B-1 cells, which are divided into two subpopulations, B-1a and B-1b[17], has been primarily elucidated in studies using the BALB/XID mouse model, which is deficient in B1-cells, especially the B-1a population[18,19].

In vitro, B-1b cells differentiate into adherent mononuclear phagocytes[20], also known as B-1 cell-derived phagocytes (henceforth termed B-1P cells here), which can be distinguished from monocytes-derived macrophages by the co-expression of lymphoid and myeloid markers (i.e., IgM^+ $CD19^+F4/80^+CD11b^+$)[21].

Previous studies have demonstrated the involvement of B-1 cells in the infection process of various pathogens, including *L. amazonensis* and other *Leishmania* species[22–24]. Interestingly, these cells respond to *L. amazonensis* infection by producing high levels of IL-10 in vitro[25,26]; however, IL-10 production in infected B-1P cells and the participation of such cells in the progression of leishmaniasis remains largely elusive.

Here we define an as yet unrecognized mechanistic role for B-1P cells in *Leishmania* infection. In vitro, we show that B-1P cells infected by *Leishmania* parasites are unable to control parasite proliferation by defective mechanisms of PV maturation associated with impaired recruitment of lysosomes carrying V-ATPase, resulting in the formation of uniquely large and non-acidic vacuoles. These events are independent of the up-regulation of *LYST/Beige* transcripts or by the production of IL-10. In vivo, we demonstrate that B-1P cells are present at the sites of infection and validate that these cells succumb to the formation of large non-acid compartments harboring parasite multiplication. Together, these results show that B-1P cells have morphologic and functional participation in the progression of *L. amazonensis* infection, revealing new immunobiological mechanisms of the host-parasite interplay with potential targets for diagnostic application and therapeutic intervention.

Materials and methods

Experimental animals

Female mice of 8 to 12-week-old C57BL/6 strain were used. The animals were kept with no water or dietary restriction, in light/dark cycles under a temperature of 22–25 °C, in the experimental animal facility at the Department of Parasitology, University of São Paulo. All experiments were carried out in accordance with international ARRIVE guidelines and in full agreement with institutional and local regulations [Brazilian Federal Law #11,794, Decree #6,899 and Normative Resolutions published by the National Council for the Control of Animal Experimentation (CONCEA)] and approved by the Institutional Animal Care and Use Committee (IACUC) under protocols #104/2013 and #95/2013 at the Institute of Biomedical Sciences, University of São Paulo, Brazil.

Bone marrow-derived macrophages isolation

Bone marrow-derived macrophages (BMM) were prepared as described[10]. Briefly, BMM from C57BL/6 mice were obtained after 7 days of bone marrow differentiation in RPMI medium (Vitrocell) supplemented with supplemented with 25 mM HEPES, 1.5 g/L sodium bicarbonate, 1 mM sodium pyruvate, 2 mM L-glutamine, 100 U/mL penicillin, 100 µg/mL streptomycin, 20% (v/v) heat-inactivated fetal bovine serum (iFBS, from Vitrocell) and 20% (v/v) L-929 cell conditioned medium, pH 7.2, at 37 °C in a 5% CO_2 standard humidified incubator.

Peritoneal macrophages and B-1P cells isolation

B-1P cells were obtained from C57BL/6 mice by using an adapted two-step differentiation protocol[20]. Step One: Peritoneal cavity cells were collected by washes with RPMI-1640 medium supplemented with 25 mM HEPES, 1.5 g/L sodium bicarbonate, 1 mM sodium pyruvate, 2 mM L-glutamine, 100 U/mL penicillin, 100 µg/mL streptomycin, without iFBS, pH 7.2. The cells were incubated for 1 h at 37 °C in a 5% CO_2 standard humidified incubator. Non-adherent cells were removed, and adherent monolayers were incubated for 5 days in RPMI medium supplemented with 10% (v/v) iFBS. Step Two: After the 5 days of incubation, the adherent cells were used as peritoneal macrophages. For B-1P cells differentiation, the cells present in the supernatant were then incubated in RPMI medium containing 10% (v/v) iFBS and 50% (v/v) L-929 cells conditioned medium for at least 24 h. The number of adhered B-1P cells (37.14% average from the total) was determined by subtracting the total peritoneal cells initially plated minus the number of non-adherent cells counted in the supernatant.

RAW cell line culture

RAW 264.7 macrophage-like cells (American Tissue Type Collection, ATCC) were maintained in RPMI medium supplemented with supplemented with 25 mM HEPES, 1.5 g/L sodium bicarbonate, 1 mM sodium pyruvate, 2 mM L-glutamine, 100 U/mL penicillin, 100 µg/mL streptomycin, 10% (v/v) iFBS, pH 7.2, at 37 °C in a 5% CO_2 standard humidified incubator. Subcultures were prepared by washing the cells twice with PBS, followed by the addition of trypsin for 5 min, then dilution in complete medium and thoroughly re-suspension.

Leishmania amazonensis parasites

Leishmania amazonensis (IFLA/BR/67/PH8) parasites were obtained from lesions in C57BL/6 mice and then propagated as promastigotes in M199 medium (Vitrocell) supplemented with 40 mM HEPES, 2.5 µg/mL hemin, 10 mM adenine, 2 mM L-glutamine, 2 µg/mL D-biotin, 100 U/mL penicillin, 100 µg/mL streptomycin and 20% (v/v) iFBS, pH 7.2, at 26 °C in a bio-oxygen demand incubator, as described[27,28]. Subcultures were made weekly at an initial density of 5×10^5 promastigotes/mL up to six passages. Parasites were washed three times in phosphate-buffered saline (PBS) before use in experiments.

In vitro infection

The cells were seeded at least 24 h prior to infection. For immunofluorescence assays, the cells were seeded on top of glass coverslips in 24-well plates. *L. amazonensis* promastigotes were added at a multiplicity of infection (MOI) of 2 in RPMI supplemented with 5% (v/v) iFBS and 2% (v/v) L-929 cell supernatant for 2 h at 34 °C in a 5% CO_2 standard humidified incubator. The cells were then washed three times with PBS to remove non-internalized parasites, followed by the addition of RPMI supplemented with 10% (v/v) iFBS and 2% (v/v) L-929 cell supernatant and incubated at 34 °C in a 5% CO_2 humidified incubator for the indicated periods.

In vivo infection and tissue processing

Wild-type and *TLR9*$^{-/-}$ mice were injected with 10^6 *L. amazonensis* stationary phase promastigotes in the left hind footpad. Lesion size progression was followed by weekly measurements with a caliper by an observer blinded to the experimental group assignments. The parasite load in the lesions was quantified by a limiting dilution assay. Footpad tissue homogenates were dissociated by incubation with collagenase (2 mg/mL, Sigma-Aldrich; St. Louis, MO) in Tyrode buffer (140 mM NaCl, 5 mM KCl, 2.5 mM $CaCl_2$, 10 mM HEPES, 2 mM $MgCl_2$, pH 7.2) for 2 h at 37 °C under mild agitation. The homogenate was filtered through a 70-mm pore-size cell strainer (Falcon®; Corning, NY), centrifuged at 20 x g for 5 min, and washed twice with PBS (230 x g for 10 min). The cellular suspension was diluted 100-fold in complete M199 media, followed by another 10-fold serial dilution in 96-well plates performed in triplicates. After 10 days of incubation at 26 °C, the presence or absence of viable parasites in each well was determined by direct observation under an inverted light microscope. Results are presented in logarithm scale in base 10 (Log_{10}) of the highest dilution in which viable promastigotes were observed. In some experiments, 2.5×10^7 amastigotes were injected in the peritoneal cavity and cells were collected by peritoneal washes with RPMI-1640 medium after 48 h of infection.

In some experiments, footpads of animals were removed and fixed in freshly made 10% formaldehyde (v/v) in PBS, followed by dehydration and paraffin embedding. Serial 5-µm sections were stained by hematoxylin and eosin (H&E, Sigma Aldrich). The histological sections were evaluated and captured under a light microscope (AxioImager M2, Zeiss) coupled with a high-resolution camera (AxioCam HRc, Zeiss).

Phenotypic characterization of B-1 and B-1P cells by flow cytometry

Cells isolated from footpad lesions, peritoneal cells, or the non-adherent cells fraction of five days of culture (B-1 cells) were counted, suspended in PBS containing 2% FBS and incubated with an anti-mouse CD16/CD32 antibodies (BD Pharmingen) to block Fc receptors, followed by staining with fluorochrome-conjugated mAb for surface markers, namely: phycoerythrin (PE)-labeled anti-mouse CD19 (Caltag Medsystems), Pacific Blue (PB)-labeled anti-mouse F4/80 (Thermo Scientific), and fluorescein isothiocyanate (FITC)-labeled anti-mouse CD23 (BD-Pharmingen). Fluorescence-minus-one (FMO) controls were used to determine the cut-off point between background fluorescence and positive populations in multicolor flow cytometry experiments. All the surface markers were incubated for 30 min at 4 °C in the dark. After washes, stained cells were fixed with 4% paraformaldehyde solution for 15 min at room temperature (RT). Cells were then washed, and incubated in PBS containing 2% SFB and then the samples were acquired by using an LSRFortessa™ flow cytometer (BD Bioscience) or an Attune Acoustic Focusing Flow Cytometer (Applied Biosystems) acquiring at least 50,000 events. Data were analyzed by using the FlowJo software, version 10.0.7 (Tree Star Inc. Ashland, OR, USA) as shown (Fig. S1).

Drug treatment in vitro

To evaluate the potential association between the susceptibility to infection with the size of PV, B-1P cells and BMM were pretreated with 1 µM of vacuolin-1 (compound 5114069, Cayman Chemical) for 1 h. The cells were then washed with fresh medium and infected. The phagocytosis capacities of B-1P cells and BMM were evaluated by pretreating the cells with 5 mM latrunculin A (Sigma-Aldrich) for 30 min at 37 °C. After the treatment, the cells were washed with fresh medium and infected on ice for 30 min to allow parasite attachment, followed by incubation of the cells at 34 °C for an additional 30 min.

Vacuole pH detection with acridine orange

Infected cells were incubated for 15 min at 34 °C with RPMI medium containing acridine orange (AO) [2 µg/mL 3,6-bis-(dimethylamino) acridine; Sigma-Aldrich] in 5% CO_2. After washes with PBS to remove excess AO,

the cells were incubated in RPMI with 5% FBS medium supplemented with 2% L-929 conditioned media, and allowed to settle at 37 °C in a 5% CO_2 humidified incubator for 30 min before imaging.

Immunofluorescence and image analyses

For the immunofluorescence assays, the samples were processed and stained using two strategies. For staining and counting, coverslips containing the infected cells were washed and fixed with 100% ice-cold methanol for 5 min. After fixation, the samples were treated with blocking and permeabilization solution [1% BSA, 0.1% saponin, and 0.1% sodium azide in 25 mM Tris-buffered saline (TBS)] for 30 min. The coverslips were incubated with anti-LAMP-1 polyclonal antibody (Developmental Studies Hybridoma Bank) followed by anti-rat IgG antibody Alexa Fluor 568-conjugated (Thermo Scientific); anti-*Leishmania* serum followed by anti-rabbit IgG antibody Alexa Fluor 488-conjugated (Thermo Scientific); PE-labeled anti-mouse CD19 (BD Bioscience); FITC-labeled anti-mouse IgM (BD Bioscience); anti-EEA-1 (BD Bioscience) polyclonal antibody followed by anti-mouse IgG antibody Alexa Fluor 488 (Thermo Scientific); and anti-V-ATPase polyclonal antibody (Anti-V-ATP6V0D2, Sigma Aldrich) followed by anti-rabbit IgG antibody Alexa Fluor 488 (Thermo Scientific). Cells were incubated with 10 µg/mL DAPI (Sigma-Aldrich) to detect the nuclei of parasites and host cells. For the assessment of phagocytosis, the samples were processed without permeabilization (staining only OUT parasites) and incubated with anti-*Leishmania* polyclonal antibody followed by anti-rabbit IgG antibody Alexa Fluor 488 and 10 µg/mL propidium iodide (PI; Sigma-Aldrich). The images were randomly acquired (an observer blinded to the experimental group assignments) in a fluorescence microscope (Leica DMI6000B/AF6000) coupled to a digital camera system (DFC365FX) moving through visual fields in parallel rows across each coverslip, and analyzed by using ImageJ. An appropriate filter set was used depending on the sample fluorescence labeling. The regions of interest (ROIs) were delineated manually to measure diameter (Fig. 3) or fluorescence intensity. The number of events analyzed is annotated in corresponding figure legends.

Additionally, vacuole pH detection with AO images was acquired in the InCell Analyzer High Content Imaging System (GE), version 2200, by using a 20x objective. The images from the Cell Analyzer High Content Imaging System were analyzed by CellProfiler software, providing the following outputs per image. Total number of cells, total number of infected cells, number of parasites per infected cell, the ratio of infected cells to the total number of cells, and intensity of Cy3 fluorescence channel per vacuole (Fig. S5).

Infection quantification

The infection quantification was performed by examining stained slides on a fluorescence microscope with an objective lens under immersion oil (Leica DMI6000B/AF6000; 100x lens). Quantification was performed on a regular basis by an investigator blinded to the group assignments. Moving through visual fields in parallel rows across each coverslip, the number of macrophages and the number of intracellular parasites was quantified with a manual click-counter. At least 300 cells per coverslip were counted. Parasite load was determined by counting the number of intracellular parasites in at least 100 infected cells. The infection index was obtained by multiplying the percentage of infection per the average number of intracellular parasites per cell. In the phagocytic capacity assay, the attached parasites (OUT) were visualized by microscopy in green and red (anti-*Leishmania* and Nuclei PI-staining, respectively), while internalized (IN) parasites were visualized only in red (Propidium iodide, PI).

Cytokine quantification

Cell culture supernatants were used for cytokines and/or nitrite quantification. IL-10 and TNF-α were assayed by using the Cytometric Bead Array (CBA) kit for Mouse inflammation (BD Biosciences). The sample acquisitions were carried out on FACSCanto II (BD Biosciences) and the data analysis was performed with the FACSDiva™ software.

Quantitative real-time PCR

The RNA extraction and purification were performed by using the Quick-RNA™ MiniPrep kit (Zymo Research). Quantification was carried out in a NanoDrop instrument (Thermo Scientific) and cDNA synthesis was performed by using a kit (SuperScript III Reverse Transcriptase, Invitrogen). Quantitative PCR reaction was performed on the equipment StepOnePlus™ Real-Time PCR System (Applied Biosystems) by using the Maxima SYBR Green/ROX qPCR Master Mix (Thermo Scientific). Oligonucleotide primers, forward: 5'-AGC AGA AGG TGA TAG ACC AGA A-3' and reverse: 5'-CCC ACA CTT GGA TCA TCA ATG C-3' were used to amplify a portion of *LYST/Beige* cDNA; and forward: 5'-TCA GTC AAC GGG GGA CAT AAA-3' and reverse: 5'-GGG GTC GTA CTG CTT AAC CAG-3' to amplify the housekeeping gene (*Hprt1*). The reaction was incubated for 10 min at 95 °C and then for 40 cycles of 15 s at 95 °C, followed by 30 s at 55 °C and 30 s at 72 °C. Fluorescence was detected at each annealing step. Technical triplicates were performed for each reaction and negative controls were included. The data were presented as relative quantification normalized by *Hprt1* expression levels calculated through the 2-ΔΔCt methodology[29].

Western blot

A total of 20 µg of protein/well were separated under reducing conditions on a 12% sodium dodecyl sulfate (SDS) polyacrylamide gel and blotted onto nitrocellulose membranes with a transfer system (BioRad Laboratories, Hercules; CA). The membranes were probed with an anti-LAMP-1 polyclonal antibody followed by peroxidase-conjugated anti-rat IgG mAb (Imuny-VBP Biotecnologia) or anti-V-ATPase polyclonal antibody (Anti-V-ATP6V0D2, Sigma Aldrich) followed by peroxidase-conjugated anti-rabbit IgG mAb (Imuny-VBP Biotecnologia). Immunoblots were developed by using the Supersignal West Pico Chemiluminescent Substrate (Thermo Scientific) and detected with a ChemiDoc Imaging System (BioRad) on the ImageLab (BioRad) software.

Statistical analysis

Data were analyzed with Prism 6.0 (GraphPad Software, San Diego, CA). Statistical significance was determined by the Student's *t*-test (two-tailed), two-way analysis of variance (ANOVA), or ANOVA one-way for data with Gaussian distribution and similar variation between groups. After the test for normal and log non-normal distribution, non-Gaussian data were analyzed by Mann-Whitney or Kruskal-Wallis, or Wilcoxon test, as indicated. Statistically significant differences were defined as * when p-values were <0.05, ** $p<0.01$ and *** $p<0.001$. Results represent means ± standard deviation (SD) or standard error of the mean (SEM) as indicated. The number of independent experiments, and technical and biological replicates are indicated in corresponding figure legends. Biological replicates mean different biological samples (e.g., different mice, different cell cultures, different protein preparations). Technical replicates mean different measurements with the same biological sample. Independent experiments are experiments performed on different days with different biological samples. The number of mice per group is annotated in the corresponding figure legends.

Results

B-1P cells are permissive to *L. amazonensis* infection in vitro

B-1 cells were isolated from the peritoneal cavity of mice as described[20]. Here we adapted an experimental two-step cell adhesion protocol (Fig. S1, A-C) to enrich the population of B-1 phagocyte precursors (B-1b cells) for the differentiation into B-1P cells in vitro (Fig. S1 D). B-1 enriched cell populations were confirmed by flow cytometry assays with specific cell surface markers (Fig. S1 E). In these defined experimental conditions, we first established the baseline infection rate and parasite multiplicity in B-1P cells, side-by-side with bone marrow-derived macrophages (BMM), the gold-standard model of infection. We observed that despite no difference in the percentage of infection between B-1P cells and BMM after 2 h of infection (Fig. 1A), parasite multiplicity in B-1P cells was almost three times higher than BMM after 48 h of infection (Fig. 1B). Immunofluorescence staining assays with specific antibodies against intracellular amastigotes or lysosomal-associated membrane protein-1 (LAMP-1) and 4′,6-diamidino-2-phenylindole (DAPI) show that B-1P cells harbor a high number of amastigotes inside of large vacuolar structures (Fig. 1C) relative to BMM (Fig. 1D).

To evaluate whether the effect in parasite multiplicity is associated with the process of invasion, either B-1P cells or BMM were first pretreated with latrunculin A (*Lat* A), which inhibits phagocytosis by preventing actin polymerization; then the number of intracellular (IN) versus extracellular parasites (OUT) was determined by using immunofluorescence staining in non-permeabilized cells (Fig. S2 A). *Lat* A treatment inhibited parasite entry in >80% of B-1P cells (Fig. 1E) and BMM (Fig. 1F), thereby suggesting that B-1P cells (similarly to macrophages) promoted *Leishmania* phagocytosis. Other similarities between B-1P cells and BMM were observed regarding the polarity of parasite entry during phagocytosis (Fig. S2, B and C) and early recruitment of intracellular vesicles, such as endosomes and lysosomes, in the biogenesis of PV (Fig. S2, D-F)[30–33]. Finally, since B-1P cells originate from B-1 cells, one of the main sources of the anti-inflammatory cytokine interleukin-10 (IL-10)[34], we also evaluated the levels of anti- or pro-inflammatory cytokines in the supernatant of B-1P cells or BMM infected cells. No detectable differences in the levels of IL-10 were observed in B-1P cells or BMM infected with *L. amazonensis* (Fig. 1G), data indicative that the susceptibility to infection of B-1P cells associated with the large PV is apparently independent of IL-10 production. In contrast, the levels of TNF-α, a pro-inflammatory cytokine involved in the defense against *Leishmania* infection[35], were markedly low in B-1P cells relative to BMM (Fig. 1H), suggesting that these cells are either unable or inefficient in their molecular response against the parasite. Other cytokines such as MCP-1 and IL-6 were also evaluated but remained at background levels (data not shown). These results indicate that B-1P cells functionally behave as conventional macrophages in the process of *Leishmania* infection; however, these cells are highly susceptible to parasite proliferation, independently of IL-10, suggesting that other mechanisms associated with the intracellular trafficking of vesicles may be involved in the biogenesis of these large *Leishmania*-PV.

PV expansion is independent of the *LYST/Beige* gene in B-1P cells

To evaluate the anatomical and functional attributes of the *Leishmania*-PV in B-1P cells, we performed a series of in vitro infection assays for microscopy and imaging analysis. First, we used a well-established method to determine the size of *Leishmania*-PV by measuring the largest diameter of the vacuole[7,36]. After 96 h of infection, the *Leishmania*-PV (arrows) grew abnormally large in B-1P cells when compared in side-by-side experiments with BMM (Fig. 2A, note schematic representation at the right side of each corresponding image), with some vacuoles reaching over 25 µm in diameter (average, 15.3 ± 0.3 µm). In contrast, the *Leishmania*-PV of infected BMM grew smaller than B-1P cells with only a few cells containing vacuoles of ~20 µm in diameter (average, 12.8 ± 0.2 µm) (Fig. 2B).

Next, to begin to evaluate the molecular mechanisms associated with these empiric observations, we analyzed the expression of the *LYST/Beige* gene, which encodes for the LYST protein responsible for regulating the size of lysosomes[37]. In macrophages, the gain- and loss-of-function of the *LYST/Beige* gene have been associated with the control of *Leishmania*-PV expansion; indeed, *LYST/Beige* upregulation markedly reduces the size of lysosomes, limiting the expansion of the *Leishmania*-PV and controlling parasite growth[7]. Thus, to investigate whether *LYST/Beige* gene is regulated in B-1P cells during *L. amazonensis* infection, total mRNA obtained from B-1P cells or BMM infected with *L. amazonensis* for 96 h was analyzed by quantitative PCR (qPCR). Surprisingly, the relative levels of *LYST/Beige* transcripts in B-1P cells (~2.8-fold) were nearly double those levels in BMM (~1.5-fold) (Fig. 2C), results indicating that B-1P cells —unlike BMM— are unable to control the expansion of *Leishmania*-PV via LYST. Moreover, to evaluate the potential association with LYST and intracellular trafficking of lysosomes, we next tested the expansion of *Leishmania*-PV in B-1P cells or BMM pretreated with vacuolin-1, a cell-permeable inhibitor of lysosomal exocytosis that causes rapid expansion of late endosomes/lysosomes[38,39] and the formation of large *Leishmania*-PV[7]. Notably, vacuolin-1 barely affected the

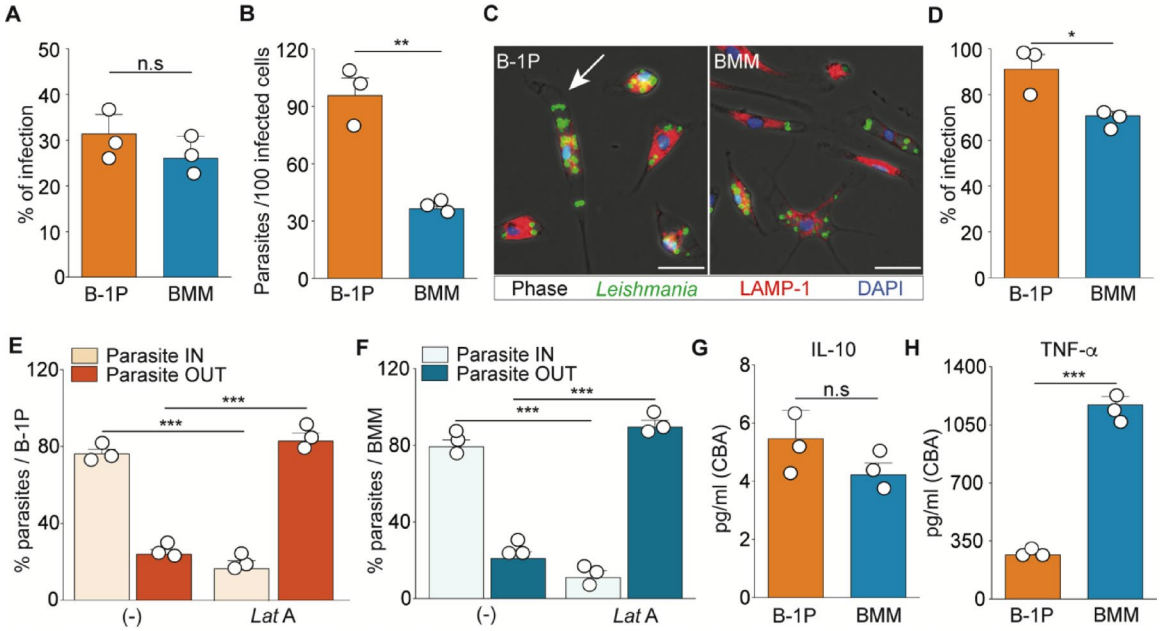

Fig. 1. B-1P cells are highly permissive to ***L. amazonensis*** proliferation. (**A**) Infection of B-1P cells and BMM for 2 h with *L. amazonensis* stationary-phase promastigotes (MOI = 2). The results are expressed as *Leishmania* per 100 infected cells and correspond to the mean ± standard deviation (SD) of three independent biological assays. No statistical significance (n.s.) was observed (Student's *t*-test). See also Fig. S1 for additional data. (**B**) *Leishmania* proliferation in B-1P cells and BMM after 48 h. The results are expressed as *Leishmania* per infected cell and correspond to the mean ± SD of triplicates. **, $p < 0.003$ (Student's *t*-test). (**C**) Representative images of the in vitro infection assay (48 h) are presented in (D) and (E). By immunofluorescence, parasites are visualized in green, PV in red (LAMP-1), and the nuclei of the cells/parasites in blue (DAPI). All the channels were merged with phase contrast. The high number of parasites contained in a PV in B-1P cells is indicated (white arrow). Scale bar, 25 µm. (**D**) Quantification of the total of infected cells (% of infection) is shown in (C). Data correspond to the mean ± SD of biological triplicate assays. *, $p < 0.0389$ (Student's *t*-test). (**E**) B-1P cells and (**F**) BMM were pre-treated with latrunculin A (*Lat* A), washed, and incubated with *L. amazonensis* promastigotes for the phagocytosis assay. The IN/OUT parasite assays were determined and expressed by the percentage of *Leishmania* in each cell. Results correspond to the mean ± SD of three independent biological assays. ***, $p < 0.0001$ (two-way ANOVA). See also Fig. S2 for additional data. (**G**) Quantification of IL-10 and (**H**) TNF-α in the culture supernatant of B-1P cells and BMM 24 h after infection with *L. amazonensis*. Results correspond to the mean ± SD of three independent biological assays. No statistical significance (n.s., $p = 0.3071$); ***, $p < 0.001$ (Student's *t*-test), respectively.

diameter of *Leishmania*-PV in B-1P cells, from 18.4 ± 4.4 µm (in non-treated cells) to 20.4 ± 4.0 µm (in treated cells) (Fig. 2D and E) with no detectable differences in the infection index (Fig. 2F); however, vacuolin-1 clearly increased the diameter of *Leishmania*-PV in BMM (from 12.6 ± 2.4 µm in non-treated cells to 18.3 ± 5.2 µm in treated cells) and the infection index (Fig. 2E and F), data indicating that expansion of *Leishmania*-PV facilitates parasite multiplication. These results suggest that in B-1P cells inherent inhibitory trafficking processes, rather than the size of lysosomes, induce the formation of abnormally large *Leishmania*-PV. Taken together, the results establish that B-1P cells are unable to control the expansion of large *Leishmania*-PV independently of the up-regulation of the *LYST/Beige* gene and confirm that the formation of large vacuolar structures accounts for parasite proliferation in B-1P cells.

Deficient recruitment of V-ATPase impairs acidification of *Leishmania*-PV in B-1P cells

During *Leishmania*-PV biogenesis, fusion with lysosomal vesicles promotes its acidification and activation of lytic enzymes to either disable or destroy intracellular parasites[40]. To investigate the acidification of *Leishmania*-PV in B-1P cells, we used the permeable fluorescent probe acridine orange (AO), which emits red fluorescence once sequestered/trapped into acidic compartments. Representative images of infected B-1P cells clearly show *Leishmania*-PV (white arrow and punctate yellow circle) with low (Fig. 3A, top panel) or high (Fig. 3A, bottom panel) AO red fluorescence signal concentrated in the PV. Under these experimental conditions, we determined the acidification of *Leishmania*-PV in B-1P cells in comparison with the murine macrophage RAW cell line after 48 h of infection. Notably, nearly half of the *Leishmania*-PV in B-1P cells were non-acidic (low AO signal), as opposed to most (~90%) of the highly acidic (high AO signal) *Leishmania*-PV in RAW cells (Fig. 3B). No difference in the number of PV per infected cell was observed (Fig. 3C). These results indicate that the process

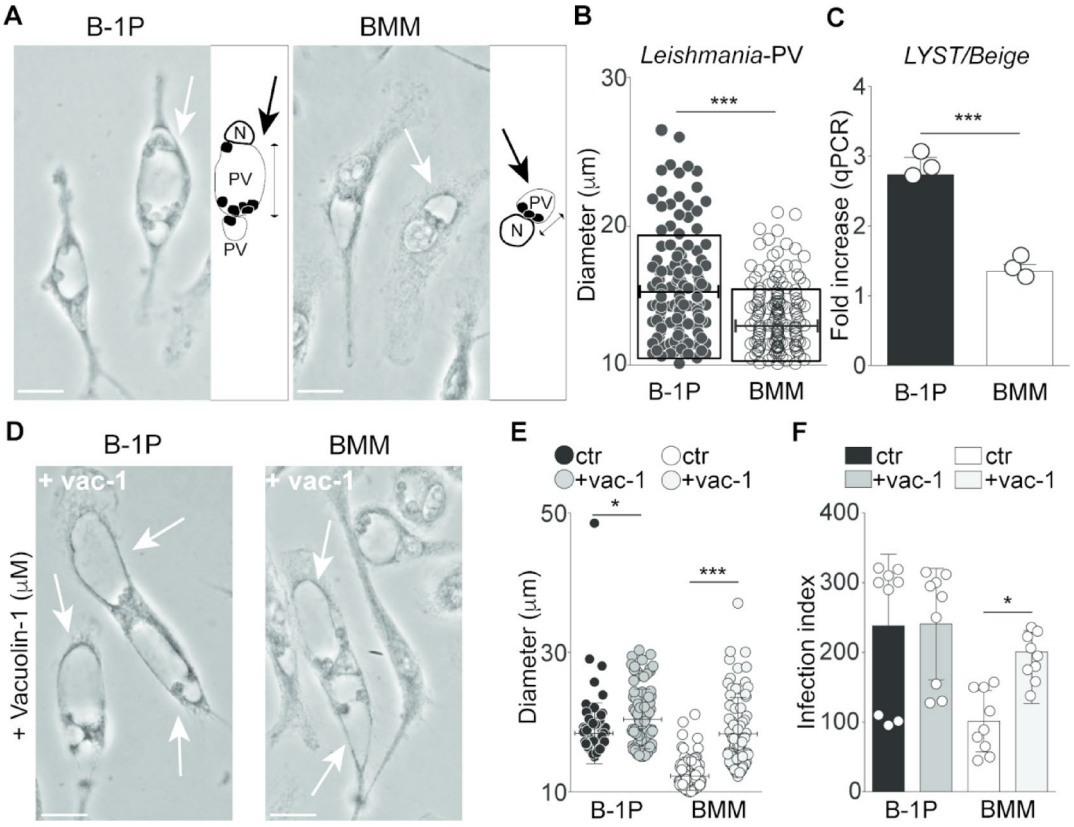

Fig. 2. Large *Leishmania*-PV in B-1P cells is independent of the ***LYST/Beige*** gene. B-1P cells and BMM were infected with stationary-phase promastigotes of *L. amazonensis* for 2 h, washed, and incubated for either 24–96 h. (**A**) Phase contrast images showing higher magnifications of *Leishmania*-containing PV in B-1P cells or BMM. Schematic representation of *Leishmania*-PV diameter measurement. Scale bar, 10 µm. (**B**) Quantification of the diameter of *Leishmania*-PV in B-1P cells and BMM, after 96 h. The values represent the mean of 80 independent PV measurements. Results correspond to the mean ± SD of three independent biological assays. ***, $p < 0.001$. (**C**) Level of *LYST/Beige* transcripts in B-1P cells and BMM analyzed by qPCR. Results correspond to the mean ± SD of three independent biological assays. ***, $p < 0.001$ (Student's *t*-test). (**D**) Representative phase contrast images showing the effect of vacuolin-1 (1 µM) in the *Leishmania*-PV (white arrows) from B-1P cells and BMM, when compared to images in (A). Scale bar, 10 µm. (**E**) Quantification of *Leishmania*-PV diameter in B-1P cells and BMM, untreated (ctr) or pretreated cells with vacuolin-1 (vac-1) and measured after 96 h of infection. The values represent the mean of 50 independent PV measurements, in each condition. Results correspond to the mean ± SD of three independent biological assays. *, $p < 0.05$; ***, $p < 0.05$ (one-way ANOVA). (**F**) Quantification of the infection index from the assay in (D). Data correspond to the mean ± SD of three independent biological assays. *, $p < 0.05$ (one-way ANOVA).

of acidification and maturation of the *Leishmania*-PV is even more defective and/or delayed in infected B-1P cells than previously reported[41]. This striking functional feature represents the first example of an entirely new mechanism of parasite resistance for long periods of infection, which has not as yet been reported for any other host cells, including but not limited to macrophages.

To further investigate the defect in the acidification of *Leishmania*-PV in B-1P cells, we next evaluated the presence of the ATP-dependent proton pump V-ATPase and the structural lysosome protein LAMP-1, a positive control for the lysosomal recruitment and acidification in *Leishmania*-PV by immunofluorescence microscopy. In these experiments, B-1P cells or BMM were infected with *L. amazonensis* for 96 h, fixed, and stained with specific antibodies to show V-ATPase recruitment to the membrane of the *Leishmania*-PV (white arrows, Fig. 3D and Fig. S3 A). In B-1P cells, V-ATPase was observed mostly spread out through the cell cytoplasm with only a few concentrated structures surrounding *Leishmania*-PV (Fig. 3D; top image, yellow arrow). In contrast, V-ATPase was clearly observed and concentrated in spots at the membrane of *Leishmania*-PV in BMM (Fig. 3D; bottom image). Given that expression of V-ATPase or LAMP-1 remained unaltered in either B-1P cells or BMM (infected or uninfected cells; Fig. S3, B and C), these data suggest that defective recruitment of V-ATPase impairs *Leishmania*-PV acidification. To demonstrate the defective recruitment of V-ATPase to the formed PV, we measured the intensity of the immunofluorescence signal of V-ATPase and LAMP-1 at the *Leishmania*-PV membrane through an imaging-based software (Fig. 3E). The defect in V-ATPase recruitment in the *Leishmania*-PV of B-1P cells was confirmed by the low-intensity fluorescence signal, compared to BMM (Fig. 3F) and to LAMP-1 (Fig. 3G), which has remained unaltered in both cells. Together the results show that

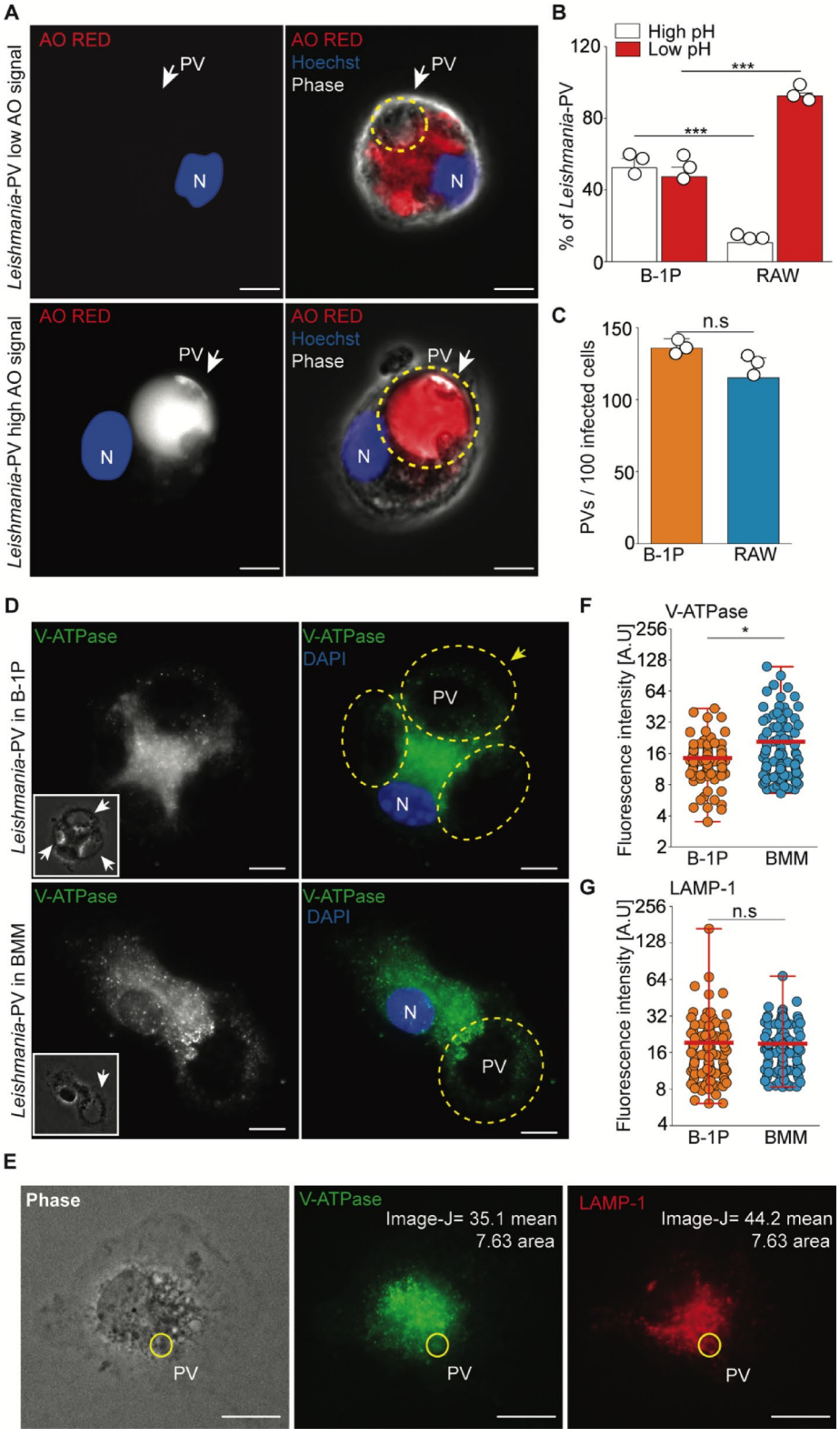

the large *Leishmania*-PV in B-1P cells are likely non-acidic or less acidic compartments due to the impaired recruitment of V-ATPase, which is the main source of acidification in BMM. These data suggest that this highly favorable microenvironment poses no selective pressure against the parasite, thereby allowing or enabling the uncontrolled proliferation of new replicative forms of *L. amazonensis*.

◀**Fig. 3**. Impaired recruitment of V-ATPase to the *Leishmania*-PV in B-1P cells. B-1P and RAW cells were infected with stationary-phase promastigotes and stained with acridine orange (AO) and Hoechst for DNA staining in live microscope imaging assays. (**A**) Representative images of B-1P cells containing *Leishmania*-PV and stained with AO and Hoechst (nuclei of cells) showing neutral/basic pH (low-AO signal) or acidic pH (high-AO signal). The panel at right represents a merged image of the AO red channel merged (at left) including the phase contrast image. White arrows and punctuated circles show *Leishmania*-PV. Scale bar, 10 µm. (**B**) Percentage of *Leishmania*-PV containing low/high pH identified in (A). Results correspond to the mean ± SD of three independent biological assays. ***, $p < 0.0004$ (two-way ANOVA). (**C**) Number of *Leishmania*-PV per 100 infected B-1P or RAW cells after 48 h of infection. No statistical significance (n.s). (**D**) Representative images of *Leishmania*-PV (PV) in B-1P cells (top images) and BMM (bottom images) showing V-ATPase (green) staining marker. In the inset, the phase contrast is shown with white arrows indicating the PV. V-ATPase image was merged with DAPI in the panel on the right. Punctuated yellow circles indicate *Leishmania*-PV; Scale bar, 5 µm. See also Fig. S3 for additional data. (**E**) Representative image of the fluorescence intensity analysis in the selected area in B-1P cells (yellow circles) corresponding to the *Leishmania*-PV, and are represented in arbitrary units (A.U.). (**F**) Quantification of the recruitment of V-ATPase or (**G**) LAMP-1 marker to the *Leishmania*-PV in B-1P cells and BMM. Results correspond to the mean ± SD of three independent biological assays. *, $p < 0.0427$ (Wilcoxon test); no statistical significance, (n.s.).

Large non-acidic *Leishmania*-PV in B-1P cells favors parasitic infection and proliferation in vivo

To evaluate the contribution of B-1P cells in the progression of *L. amazonensis* cutaneous lesions in vivo, we infected C57BL/6 mice footpads and, after five weeks post-infection, the lesions were dissected, and the tissue processed for histology and flow cytometry. Representative images of the H&E-stained section of mice footpad lesions show the number of infected cells containing parasites inside large *Leishmania*-PV (Fig. 4A). To identify the surface phenotype of the infected cells, the footpad lesions were processed and stained for flow cytometry. The cells were analyzed with specific antibodies and subclassified into two main populations: B-1P cells ($CD45^+F4/80^+CD19^+$) or macrophages ($CD45^+F4/80^+CD19^-$) from the absolute number of cells obtained from the lesions (Fig. S4 A). As expected, most of the cells (~75%) of the cells obtained from the footpad were classified as macrophages ($F4/80^+CD19^-$); however, ~25% of the cells were classified as $F4/80^+$ $CD19^+$, an indication of the presence of B-1P cells in the cutaneous lesion of *L. amazonensis* (Fig. 4B). These results are further supported by the identification of $F4/80^+$ $CD19^+$ B-1P cells from the footpads of infected mice that are genetically deficient in Toll-like receptor-9 ($TLR9^{-/-}$) (Fig. 4C), which are known to control the recruitment of macrophages to the site of lesions[10], but still develop small inflammatory lesions. The presence of B-1P cells in $TLR9^{-/-}$ infected mice suggests that the migration of these cells to sites of infection may be independent of the recruitment of monocyte-derived macrophages; thus, we reasoned that B-1P cells may be important for parasite multiplication together with infected macrophages.

To further validate our observations, we adopted another experimental model of infection in which *Leishmania* parasites were injected directly into the peritoneal cavity, the main site of resident B-1 cells in mice[15]. The rationale for this approach was to enrich the population of B-1P cells targeted by the parasites and to evaluate the development of the infection in these cells ex vivo. Indeed, we observed an increase in the number of B-1P cells upon infection, with no difference in the number of peritoneal macrophages (PM) (Fig. 4D), therefore confirming that B-1P cells are either recruited or differentiated from the precursor B-1 cells at the site of infection in vivo (as previously observed in the context of the footpad infection model).

After 48 h of infection, cells from the peritoneal cavity were recovered and analyzed by flow cytometry. Three main cell populations were identified according to the expression of CD19 and F4/80 surface markers: $F4/80^+CD19^+$ (B-1P cells), $F4/80^+CD19^-$ (macrophages), and $F4/80^-CD19^+$ (B-1 cells) (Fig. 4E). To further analyze the B-1P cells and macrophage population ex vivo, the cells were subsequently stained with AO and analyzed by fluorescence microscopy. The cells were also co-stained with anti-IgM antibody, which is an exclusive B cell marker and clearly differentiates B-1P cells from PM (Fig. 4F). Next, we compared the acidification profile of B-1P cells or PM, either infected (I) or not-infected (NI) by the parasites injected in the peritoneal cavity, by calculating the intensity of the corrected total cell fluorescence (CTCF) coefficients of AO in each cell population (Fig. S4, B and C). Notably, no changes in acidity were observed in B-1P cells either infected or non-infected by the parasite (Fig. 4G), as opposed to the increased acidification observed in PM infected by the parasite (Fig. 4H). Moreover, we also used an independent automated imaging software analysis tool (Operetta High Content Imaging System; Fig. S5) to evaluate whether the infection index (assessed by the staining the nucleus of the cell and the parasites – green fluorescence FITC channel) in either B-1P cells or BMM was associated to *Leishmania*-PV acidification (assessed by the AO dye – red fluorescence Cy3 channel) (Fig. 5A). By using a similar approach, except by infecting the differentiated cells obtained from the peritoneal cavity in vitro, we observed that the number of parasites per infected cell (Fig. 5B) and the infection rate (Fig. 5C) were higher in B-1P cells, which presented less acidification (fluorescence intensity) in the *Leishmania*-PV, when compared to BMM (Fig. 5D). Together, these results show that B-1P cells containing less acidic PV favor high *Leishmania* infection rate, presumably by the lack or defective mechanisms of intracellular trafficking.

Finally, we used the ex-vivo infected cells to evaluate the recruitment of V-ATPase and LAMP-1 to the *Leishmania*-PV by using immunofluorescence microscopy. As previously observed in vitro, the V-ATPase signal

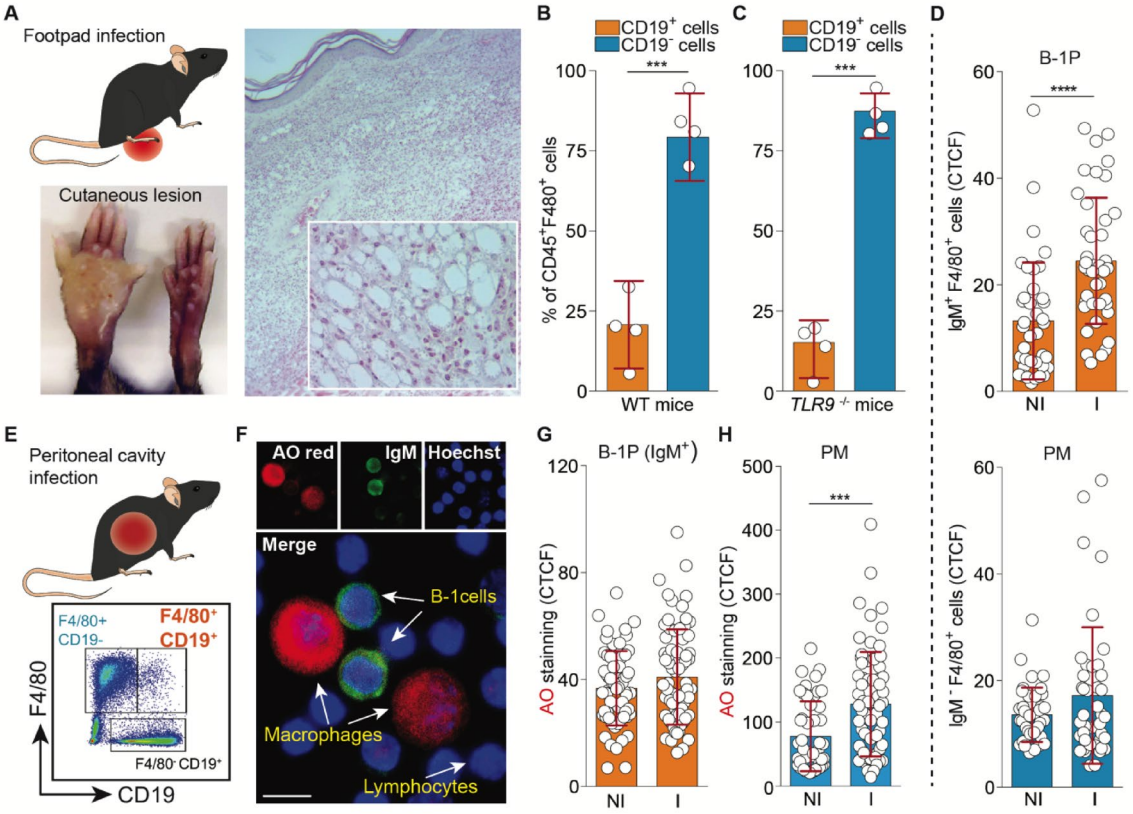

Fig. 4. B-1P cells are recruited to cutaneous lesions in vivo. (**A**) Representative image of the lesions and a histological section of an infected footpad during the course of C57BL/6 mice infection with *L. amazonensis*. The inset image shows large *Leishmania*-PV of different cells within the infected tissue. (**B**) Normalized percentage of $CD45^+F4/80^+$ populations presenting B-1P cells ($CD19^+$ cells) or macrophages ($CD19^-$ cells) from infected wild-type (WT) mice with *L. amazonensis*. Different cell populations obtained from footpad lesions were analyzed by flow cytometry and represented as the percentage of total cells. Results correspond to the mean ± SD ($n = 4$). ***, $p < 0.001$ (Student's *t*-test). (**C**) Normalized percentage of $CD45^+F4/80^+$ populations presenting B-1P cells ($CD19^+$ cells) or macrophages ($CD19^-$ cells) from infected *TLR9*$^{-/-}$ mice with *L. amazonensis*. Results correspond to mean ± SD ($n = 4$). ***, $p < 0.001$ (Student's *t*-test). (**D**) Total cell fluorescence intensity (CTCF) for the presence B-1P cells (IgM^+) or PM (IgM^-) cell populations in comparison with non-infected (NI) or infected (I) samples from the peritoneal cavity. At least 50 cells were analyzed by using Image J software. Results correspond to the mean ± SD. ****, $p < 0.0001$ (Student's *t*-test). (**E**) Flow cytometry analysis of the B-1P cells ($F4/80^+CD19^+$) cell population 48 h after *Leishmania* infection in the peritoneal cavity of C57BL/6 mice. (**F**) Peritoneal cells were stained with AO, IgM-FITC, and Hoechst. B-1P cells (IgM^+), macrophages (IgM^-), and lymphocytes (IgM^- and small nuclei) were visualized in the representative image. Scale bar, 10 µm. (**G**) B-1P cells and (**H**) Ex-vivo analysis obtained from the peritoneal cavity of infected mice. The cells were stained and analyzed in Image J software measuring the corrected total cell fluorescence intensity (CTCF) and AO in different cell populations. At least 50 cells were analyzed. Results correspond to the mean ± SD. ***, $p = 0.0003$ (Student's *t*-test). See also Fig. S4 for additional data.

in *Leishmania*-PV (white circle) is markedly reduced in infected B-1P cells (IgM^+ staining) and in sharp contrast with the representative peritoneal macrophages (PM) displayed in the same image (IgM^- staining) (Fig. 5E). The relative quantification of the V-ATPase/LAMP-1 ratio indicates low co-localization of V-ATPase with LAMP-1 confirming the in vitro observations that B-1P cells are defective in recruiting V-ATPase to newly formed *Leishmania*-PV. In summary, our in vivo data indicate that (i) B-1P cells are indeed recruited to differential sites of infection regardless of anatomical location (e.g., footpad or peritoneal cavity); that (ii) these cells are infected by the parasite, and that (iii) the parasites reside and proliferate in large non-acidic vacuoles that are formed upon the deficiency in recruiting V-ATPase. These functional results in vivo are entirely consistent and strongly supported by our in vitro analysis showing that infection of B-1P cells by *L. amazonensis* favors parasite replication and survival and therefore has a mechanistic role in the progression of cutaneous lesions in vivo.

Discussion

While B cells play an essential role during infection by different pathogens, including *Leishmania*[25,42], the specific role of B-1P cells, an exclusive subtype of B cells, is still poorly understood. Here, we show for the first

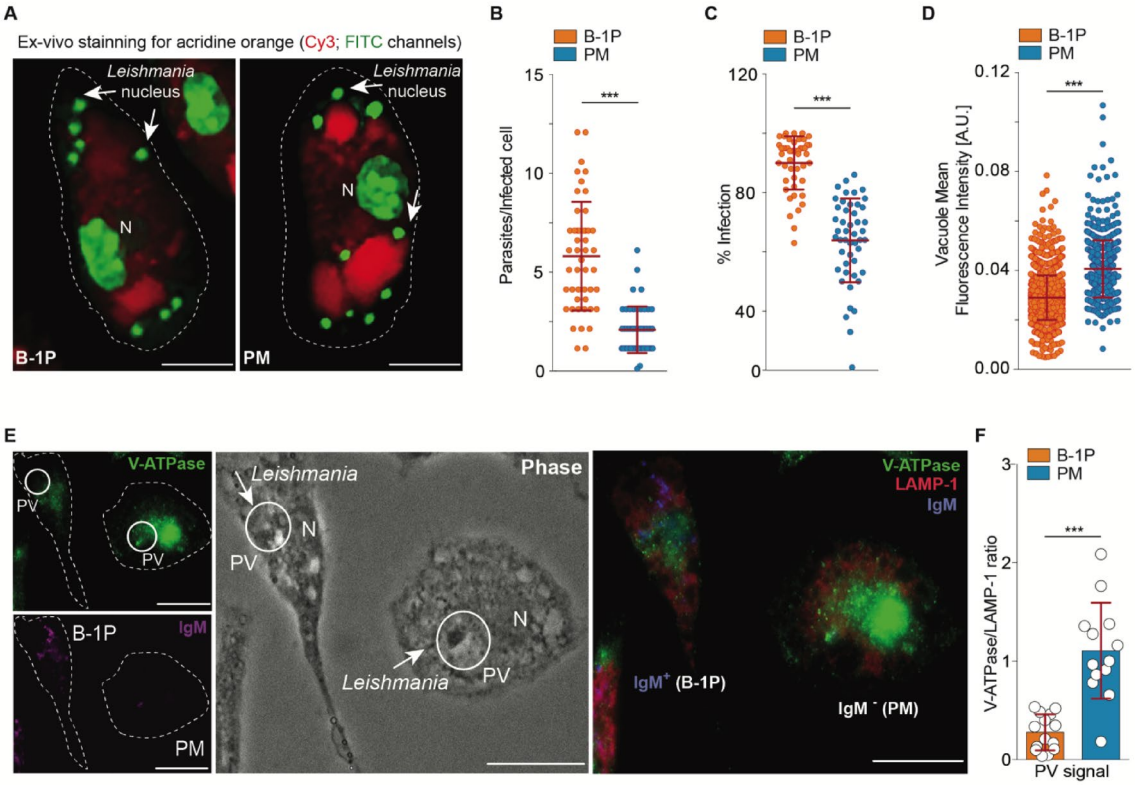

Fig. 5. Impaired recruitment of V-ATPase is associated with non-acidic ***Leishmania***-PV in B-1P cells in vivo. (**A**) Representative images of either B-1P cells or peritoneal macrophages (PM) infected with *Leishmania* amastigotes and stained with AO. The images were acquired in the InCell Analyzer High Content Imaging System by using two fluorescence channels: FITC (DNA and RNA) and Cy3 (acidic compartments). The merge channel images are shown. N: cell nucleus; white arrows: *Leishmania* nucleus. Scale bar, 10 µm. See also Fig. S5 for additional data. (**B**) The scatter plot shows the mean number of parasites/infected cells. Each circle represents an individual field, and bars are mean ± SD of technical replicates. ***, $p < 0.0001$ (Mann-Whitney test). (**C**) The scatter plot shows the percentage of infection. Each circle represents an individual field, and bars are the mean ± SD of technical replicates. ***, $p < 0.0001$ (Mann-Whitney test). (**D**) The scatter plot shows vacuole mean fluorescence intensity (A.U.) in the Cy3 fluorescence channel. Each circle represents an individual vacuole, and bars are the mean ± SD of technical replicates. ***, $p < 0.0001$ (Mann-Whitney test). (**E**) Representative images showing infected cells containing *Leishmania*-PV (white circle) stained for V-ATPase (green) and for IgM (purple signal). Parasites (white arrows) inside PV (white circle) by phase contrast and immunofluorescence staining merge (including LAMP-1 staining in red) showing infected B-1P cells (IgM^+) and PM (IgM^-) from the same representative image is showed. Scale bar, 10 µm. (**F**) *Leishmania*-PV areas were selected in a random and blinded fashion for analysis of the ratio of the fluorescence intensity for V-ATPase/LAMP-1. Results correspond to the mean ± SD of replicates. ***, $p < 0.0001$ (Student's *t*-test).

time that B-1P cells are highly susceptible to parasite infection by their endogenous inability to regulate the size and acidification of *Leishmania amazonensis*-PV. The deficiency in reducing intracellular vesicle fusion via the *LYST/Beige* gene —combined with the impaired recruitment of lysosome containing V-ATPase— results in the formation of large and non-acid *Leishmania*-PV, which favors parasitic survival and proliferation. Even though for many other species of *Leishmania*, the role of B-1P cells remains an open question to be addressed in future work, this functional discovery sheds light on an as yet unknown mechanism of cellular susceptibility to intracellular pathogens in mammalian hosts.

In general, mammalian hosts have evolved to resist parasite infection through multiple mechanisms such as nitric oxide (NO) production, secretion of inflammatory cytokines, and the formation of acidic and hydrolytic vacuolar structures that control parasite proliferation[43–45]. On the other hand, parasites such as *L. amazonensis* have co-evolved to escape these defense mechanisms by expanding these structures into large vacuoles that attenuate the deleterious effect of hydrolysis and low pH in parasite survival. Another sophisticated example of this host-parasite functional interplay is a mechanism adopted by *Leishmania* to inhibit the microbicidal response of macrophages via modulation of the CD200/CD200R signaling pathways[9,10]. In B-1P cells, the impairment of *Leishmania*-PV acidification allows for parasite multiplication, thus suggesting that the potential encounter of parasites with these cells would favor disease progression, perhaps even in the most severe forms of leishmaniasis. This concept is further supported by

recent findings showing infiltrating CD19⁺ B cells[13] in lesions derived from human patients with diffuse cutaneous leishmaniasis (DLC).

Although differences in PV maturation have been documented in other cells such as neutrophils, DCs, or monocytes[46], the defective attributes of B-1P cells, exploited by the *L. amazonensis* to facilitate survival and replication, appear to serve as an as yet unrecognized mechanism of parasite evasion. A potential non-mutually exclusive explanation is that the phagocytosis in these cells might represent an ancient cellular mechanism, which—for unknown evolutionary reasons—has not developed toward host protection. During the B-1 transition to phagocytes, the cells acquire genetic and morphological macrophage-like signatures such as F4/80. Therefore, it is plausible that these cells may also express other important ligands (e.g., MerTK, or CD36), which are known to be associated with phagocytosis[47,48]. If confirmed, these receptors could be partially responsible for the lack or blockage in signaling pathways molecules that connect with the PV maturation machinery[49]. The characterization of surface cell markers for the B-1P cells may unravel the connection with a defective PV maturation on this cell subset and its role in other pathogen infections. Recently, it has been shown that the severe acute respiratory syndrome coronavirus 2 (SARS-COV-2) inhibits autophagosome-lysosome fusion[50] and egress from cells exploiting unconventional de-acidified lysosomes with inactive degradation enzymes[51]. Nevertheless, further studies will shed light on the function of B-1P cells as phagocytes by identifying membrane receptors, which are critical for the biological function of these cells.

While changes in acidity conditions within the PV are critical for pathogen killing and antigen presentation via major histocompatibility complex (MHC) in macrophages[52], both features are paradoxically either unknown or absent in this specific B cell subtype. Indeed, the *LYST/Beige* gene up-regulation might suggest that B-1P cells, like macrophages, can control intracellular trafficking pathways to contain *Leishmania*-PV expansion. However, these cells were not only unable to control the formation of abnormally large vacuoles but also inefficient in promoting the recruitment and fusion of acidic vesicles containing V-ATPase to newly formed *Leishmania*-PV. Given that B-1P cells originate from residual B-1 cells, it is tempting to speculate that modifications in the cytoskeleton network during the transition into phagocytic-like cells could interfere with the intracellular trafficking of vesicles, especially the lysosomes containing V-ATPase, which are required for acidification[53]. Another plausible explanation would be the contribution of recycling endosome/lysosomes or Golgi-derived vesicles, which could facilitate the formation of large and underdeveloped phagosome[54–56].

Another intriguing aspect in *Leishmania* biology is the different phenotypes of the PV sizes from certain *Leishmania* species such as *L. amazonensis* compared to *L. chagasi*, the latter associated with visceral leishmaniasis (also called "kala-azar"), an often lethal form of the disease if left untreated. More relevant is the fact that *L. chagasi* proliferates inside phagocytic cells in individual PV, suggesting differential mechanisms of PV biogenesis[57] when compared to *L. amazonensis* PV. Previous data show that B-1 cells play an essential role in the host susceptibility to *L. chagasi* infection[22], with an essential function for IL-10 in this process. However, it remains unclear whether IL-10 production is sustained after transitioning to B-1P cells and upon infection with the parasite. Notably, the in vitro data presented here suggest that these cells are likely similar to macrophages than B cells.

Finally, to obtain mechanistic insights and to explore the potential role of B-1P cells in the infection in vivo, we used two models of infection where we unequivocally show that these cells are indeed recruited to the site of lesion and targeted by the parasite, therefore suggesting a central, if as yet unappreciated, role of B-1P cells in disease progression. Although the presence of B-1 cells in inflammatory sites has been demonstrated during infection[58], it is the first time that a mechanistic role of deficiency in PV maturation has been proposed to explain the susceptibility of these cells to infection and permissiveness to parasite growth.

Other aspects merit further discussion. First, this experimental evidence is also supported by an infection model in BALB/XID mice, which are naturally deficient in B-1 cells and therefore are resistant to infection by different *Leishmania* species[22,23]. Second, one should note that in cutaneous leishmaniasis, T-lymphocytes, and activated macrophages are responsible for controlling the infection[59]; however, in DCL, the lesions are constituted by unresponsive T-lymphocytes surrounded by a much higher number of infected macrophages[60], and a marked plasma cell infiltration[61]. Because we show that B-1P cells migrate to inflammatory sites where they would trigger an anti-inflammatory response[62–64], one might also speculate that the results reported here could represent a novel role of these cells, not only by allowing parasite infection and proliferation but also perhaps by contributing to the overall spread of the disease. On another line of investigation, our group has previously reported that the presence of B-1 cells is associated with malignant melanoma biology, mediated by the cell-to-cell adhesion through the melanoma cell adhesion molecule (MCAM, also known as MUC18 or CD146), by which the presence of this specific cell population promotes tumor progression and metastasis in murine models and human patients[65], data attesting to the functional relevance of B-1 cells not only in human parasitology but also in cancer biology.

In conclusion, here we show that B-1P cells create an internal environment with reduced acidification and impaired recruitment of V-ATPase. We highlight a heretofore-unrecognized function of B-1P cells as alternative susceptible target cells for the intracellular parasite *L. amazonensis*, with differential morphologic and functional attributes from resident macrophages, which is bound to have translational implications in mechanism-based therapeutic strategies and for medical parasitology at large. Future studies shall determine the full biological and clinical relevance of B-1 lymphocytes or B-1P cells in ulcerative or nodular lesions from unfortunate human patients affected by leishmaniasis worldwide.

Data availability

The data that support the findings of this study are available from the corresponding author upon reasonable request.

Received: 23 January 2025; Accepted: 19 August 2025
Published online: 29 September 2025

References

1. Reithinger, R. et al. Cutaneous leishmaniasis. *Lancet Infect. Dis.* **7**, 581–596 (2007).
2. Convit, J. & Ulrich, M. Antigen-specific immunodeficiency and its relation to the spectrum of American cutaneous leishmaniasis. *Biol. Res.* **26**, 159–166 (1993).
3. Dostalova, A. & Volf, P. *Leishmania* development in sand flies: Parasite-vector interactions overview. *Parasit. Vectors*. **5**, 276 (2012).
4. Dermine, J. F., Scianimanico, S., Prive, C., Descoteaux, A. & Desjardins, M. *Leishmania* promastigotes require lipophosphoglycan to actively modulate the fusion properties of phagosomes at an early step of phagocytosis. *Cell. Microbiol.* **2**, 115–126 (2000).
5. Vinet, A. F., Fukuda, M., Turco, S. J. & Descoteaux, A. The *Leishmania donovani* lipophosphoglycan excludes the vesicular proton-ATPase from phagosomes by impairing the recruitment of synaptotagmin V. *PLoS Pathog.* **5**, e1000628 (2009).
6. Ndjamen, B., Kang, B. H., Hatsuzawa, K. & Kima, P. E. *Leishmania* parasitophorous vacuoles interact continuously with the host cell's Endoplasmic reticulum; parasitophorous vacuoles are hybrid compartments. *Cell. Microbiol.* **12**, 1480–1494 (2010).
7. Wilson, J. et al. Control of parasitophorous vacuole expansion by lyst/beige restricts the intracellular growth of *Leishmania amazonensis*. *PLoS Pathog.* **4**, e1000179 (2008).
8. Ji, X., Chang, B., Naggert, J. K. & Nishina, P. M. Lysosomal trafficking regulator (LYST). *Adv. Exp. Med. Biol.* **854**, 745–750 (2016).
9. Cortez, M. et al. *Leishmania* promotes its own virulence by inducing expression of the host immune inhibitory ligand CD200. *Cell. Host Microbe*. **9**, 463–471 (2011).
10. Sauter, I. P. et al. TLR9/MyD88/TRIF signaling activates host immune inhibitory CD200 in *Leishmania* infection. *JCI Insight*. **4** (10), e126207 (2019).
11. Rossi, I. V. et al. Extracellular vvesicles during tritryps infection: complexity and future challenges. *Mol. Immunol.* **132**, 172–183 (2021).
12. Kaye, P. & Scott, P. Leishmaniasis: complexity at the host-pathogen interface. *Nat. Rev. Microbiol.* **9**, 604–615 (2011).
13. Christensen, S. M. et al. Host and parasite responses in human diffuse cutaneous leishmaniasis caused by *L. amazonensis*. *PLoS Negl. Trop. Dis.* **13**, e0007152 (2019).
14. Baumgarth, N., Tung, J. W. & Herzenberg, L. A. Inherent specificities in natural antibodies: a key to immune defense against pathogen invasion. *Springer Semin Immunopathol.* **26**, 347–362 (2005).
15. Montecino-Rodriguez, E. & Dorshkind, K. New perspectives in B-1 B cell development and function. *Trends Immunol.* **27**, 428–433 (2006).
16. O'Garra, A. et al. Ly-1 B (B-1) cells are the main source of B cell-derived Interleukin 10. *Eur. J. Immunol.* **22**, 711–717 (1992).
17. Haas, K. M. B-1 lymphocytes in mice and nonhuman primates. *Ann. N Y Acad. Sci. Dec.* **1362**, 98–109 (2015).
18. Rawlings, D. J. et al. Mutation of unique region of bruton's tyrosine kinase in immunodeficient XID mice. *Science* **261**, 358–361 (1993).
19. Riggs, J. et al. X-chromosome-linked immune-deficient mice have B-1b cells. *Immunology* **108**, 440–451 (2003).
20. Almeida, S. R. et al. Mouse B-1 cell-derived mononuclear phagocyte, a novel cellular component of acute non-specific inflammatory exudate. *Int. Immunol.* **13**, 1193–1201 (2001).
21. Popi, A. F. et al. Co-ordinated expression of lymphoid and myeloid specific transcription factors during B-1b cell differentiation into mononuclear phagocytes in vitro. *Immunology* **126**, 114–122 (2009).
22. Arcanjo, A. F. et al. Dependency of B-1 cells in the maintenance of Splenic interleukin-10 producing cells and impairment of macrophage resistance in visceral leishmaniasis. *Front. Microbiol.* **8**, 978 (2017).
23. Arcanjo, A. F. et al. B-1 cells modulate the murine macrophage response to *Leishmania* major infection. *World J. Biol. Chem.* **8**, 151–162 (2017).
24. Gonzaga, W. F. K. M. et al. Evaluation of experimental infection with *L.* (*L.*) *amazonensis* in X-linked immunodeficient mice. *J. Parasitol.* **103**, 708–717 (2017).
25. Geraldo, M. M. et al. In vivo and in vitro phagocytosis of *Leishmania* (*Leishmania*) *amazonensis* promastigotes by B-1 cells. *Parasite Immunol.* **38**, 365–376 (2016).
26. Gonzaga, W. F., Xavier, V., Vivanco, B. C., Lopes, J. D. & Xander, P. B-1 cells contribute to susceptibility in experimental infection with *Leishmania* (*Leishmania*) *Chagasi*. *Parasitology* **142**, 1506–1515 (2015).
27. Ferreira, T. C. S. et al. Effect of DODAB nano-sized cationic bilayer fragments against *Leishmania amazonensis*. *Molecules* **5** (23), 5741 (2020).
28. Luczywo, A. et al. Microwave-assisted synthesis of 2-styrylquinoline-4-carboxylic acid derivatives to improve the toxic effect against *Leishmania* (*Leishmania*) *amazonensis*. *J. Heterocycl. Chem.* **58**, 822–832 (2021).
29. Livak, K. J. & Schmittgen, T. D. Analysis of relative gene expression data using real-time quantitative PCR and the 2(-Delta delta C(T)) method. *Methods* **25**, 402–408 (2001).
30. Courret, N. et al. Biogenesis of *Leishmania*-harbouring parasitophorous vacuoles following phagocytosis of the metacyclic promastigote or amastigote stages of the parasites. *J. Cell. Sci.* **115**, 2303–2316 (2002).
31. Forestier, C. L., Machu, C., Loussert, C., Pescher, P. & Spath, G. F. Imaging host cell-*Leishmania* interaction dynamics implicates parasite motility, lysosome recruitment, and host cell wounding in the infection process. *Cell. Host Microbe*. **9**, 319–330 (2011).
32. Rodriguez, N. E., Gaur Dixit, U., Allen, L. A. & Wilson, M. E. Stage-specific pathways of *Leishmania infantum Chagasi* entry and phagosome maturation in macrophages. *PLoS One*. **6**, e19000 (2011).
33. Uezato, H. et al. The attachment and entry of *Leishmania* (*Leishmania*) *major* into macrophages: observation by scanning electron microscope. *J. Dermatol.* **32**, 534–540 (2005).
34. Popi, A. F., Lopes, J. D. & Mariano, M. Interleukin-10 secreted by B-1 cells modulates the phagocytic activity of murine macrophages in vitro. *Immunology* **113**, 348–354 (2004).
35. Liew, F. Y., Parkinson, C., Millott, S., Severn, A. & Carrier, M. Tumour necrosis factor (TNF alpha) in leishmaniasis. I. TNF alpha mediates host protection against cutaneous leishmaniasis. *Immunology* **69**, 570–573 (1990).
36. Real, F. & Mortara, R. A. The diverse and dynamic nature of *Leishmania* parasitophorous vacuoles studied by multidimensional imaging. *PLoS Negl. Trop. Dis.* **6**, e1518 (2012).
37. Ward, D. M., Griffiths, G. M., Stinchcombe, J. C. & Kaplan, J. Analysis of the lysosomal storage disease Chediak-Higashi syndrome. *Traffic* **1**, 816–822 (2000).
38. Cao, Q., Yang, Y., Zhong, X. Z. & Dong, X. P. The lysosomal Ca^{2+} release channel TRPML1 regulates lysosome size by activating calmodulin. *J. Biol. Chem.* **292**, 8424–8435 (2017).
39. Huynh, C. & Andrews, N. W. The small chemical vacuolin-1 alters the morphology of lysosomes without inhibiting Ca^{2+}-regulated exocytosis. *EMBO Rep.* **6**, 843–847 (2005).
40. Fairn, G. D. & Grinstein, S. How nascent phagosomes mature to become phagolysosomes. *Trends Immunol.* **33**, 397–405 (2012).

41. Vinet, A. F. & A Descoteaux *Leishmania donovani* induit Un Défaut d'acidification du phagosome [*Leishmania donovani* delays phagolysosomal acidification]. *Med. Sci. (Paris)*. **26**, 227–228 (2010).
42. Popi, A. F., Zamboni, D. S., Mortara, R. A. & Mariano, M. Microbicidal property of B1 cell derived mononuclear phagocyte. *Immunobiology* **214**, 664–673 (2009).
43. Afrin, F., Khan, I. & Hemeg, H. A. *Leishmania*-host interactions - An epigenetic paradigm. *Front. Immunol.* **10**, 492 (2019).
44. Mittra, B. et al. Iron uptake controls the generation of *Leishmania* infective forms through regulation of ROS levels. *J. Exp. Med.* **210**, 401–416 (2013).
45. Santos-Pereira, S., Cardoso, F. O., Calabrese, K. S. & do Valle, T. Zaverucha. *Leishmania amazonensis* resistance in murine macrophages: Analysis of possible mechanisms. *PLoS One* **14**, e0226837 (2019).
46. Foote, J. R., Patel, A. A., Yona, S. & Segal, A. W. Variations in the phagosomal environment of human neutrophils and mononuclear phagocyte subsets. *Front. Immunol.* **10**, 188 (2019).
47. DeBerge, M. et al. MerTK cleavage on resident cardiac macrophages compromises repair after myocardial ischemia reperfusion injury. *Circ. Res.* **121**, 930–940 (2017).
48. Okuda, K. et al. Leishmania amazonensis engages CD36 to drive parasitophorous vacuole maturation. *PLoS Pathog*. **12**, e1005669 (2016).
49. Barry, A. O. et al. Impaired stimulation of p38α-MAPK/Vps41-HOPS by LPS from pathogenic *Coxiella burnetii* prevents trafficking to microbicidal phagolysosomes. *Cell. Host Microbe*. **12**, 751–763 (2012).
50. Miao, G. et al. ORF3a of the COVID-19 virus SARS-CoV-2 blocks HOPS complex-mediated assembly of the SNARE complex required for autolysosome formation. *Dev. Cell.* **56**, 427–442 (2021).
51. Ghosh, S. et al. β-coronaviruses use lysosomes for egress instead of the biosynthetic secretory pathway. *Cell* **183**, 1520–1535 (2020).
52. Aderem, A. Phagocytosis and the inflammatory response. *J. Infect. Dis.* **187** (Suppl 2), S340–345 (2003).
53. Kissing, S. et al. Vacuolar ATPase in phagosome-lysosome fusion. *J. Biol. Chem.* **290**, 14166–14180 (2015).
54. Saffi, G. T. & Botelho, R. J. Lysosome fission: planning for an exit. *Trends Cell. Biol.* **8**, 635–646 (2019).
55. Vashi, N., Andrabi, S. B., Ghanwat, S., Suar, M. & Kumar, D. Ca2+-dependent focal exocytosis of Golgi-derived vesicles helps phagocytic uptake in macrophages. *J. Biol. Chem.* **292**, 5144–5165 (2017).
56. Yu, L. et al. Termination of autophagy and reformation of lysosomes regulated by mTOR. *Nature* **465**, 942–946 (2010).
57. Hsiao, C. H. et al. The effects of macrophage source on the mechanism of phagocytosis and intracellular survival of *Leishmania*. *Microbes Infect.* **13**, 1033–1044 (2011).
58. Waffarn, E. E. et al. Infection-induced type I interferons activate CD11b on B-1 cells for subsequent lymph node accumulation. *Nat. Commun.* **6**, 8991 (2015).
59. Cunha, C. F. et al. Cytotoxic cell involvement in human cutaneous leishmaniasis: assessments in active disease, under therapy and after clinical cure. *Parasite Immunol.* **38**, 244–254 (2016).
60. Franca-Costa, J. et al. Exposure of phosphatidylserine on *Leishmania amazonensis* isolates is associated with diffuse cutaneous leishmaniasis and parasite infectivity. *PLoS One*. **7**, e36595 (2012).
61. Tasew, G. et al. Systemic FasL and TRAIL neutralisation reduce leishmaniasis induced skin ulceration. *PLoS Negl. Trop. Dis.* **4**, e844 (2010).
62. Baumgarth, N., Waffarn, E. E. & Nguyen, T. T. Natural and induced B-1 cell immunity to infections raises questions of nature versus nurture. *Ann. N Y Acad. Sci.* **1362**, 188–199 (2015).
63. Geherin, S. A. et al. IL-10^{+} innate-like B cells are part of the skin immune system and require alpha4beta1 integrin to migrate between the peritoneum and inflamed skin. *J. Immunol.* **196**, 2514–2525 (2016).
64. Martin, F., Oliver, A. M. & Kearney, J. F. Marginal zone and B1 B cells unite in the early response against T-independent blood-borne particulate antigens. *Immunity* **14**, 617–629 (2001).
65. Staquicini, F. I. et al. A subset of host B lymphocytes controls melanoma metastasis through a melanoma cell adhesion molecule/MUC18-dependent interaction: evidence from mice and humans. *Cancer Res.* **68**, 8419–8428 (2008).

Acknowledgements

We thank Dr. Nobuko Yoshida for insightful discussions and critical reading of the draft and Dr. Helen Pickersgill (Life Science Editors) for the professional editing of the manuscript. We also thank Noemi Naomi N. Taniwaki for the histology staining services, Joelcimar Martins da Silva, and the Core Facility for Scientific Research of the University of São Paulo (CEFAP-USP/CONFOCAL- Confocal Microscopy and Cell Culture Laboratory) for the InCell Analyzer High Content Imaging System analysis. This work was funded in part by Brazilian Funding Agencies from the São Paulo State Research Support Foundation (FAPESP Grant; #2012/24105-3, #2020/13562-0, #2024/05757-7), National Council for Scientific and Technological Development (CNPq, Grant #443816/2014-0) and the Coordination for the Improvement of Higher Education Personnel (CAPES; Finance Code #001)—all to MC. RP and WA received serial research awards from the Levy-Longenbaugh Donor-Advised Fund. NSF was a Research Fellow of CNPq; TCSF, and DBA are Research Fellows of CAPES, and IPS was from FAPESP (#2013/14087-0).

Author contributions

N.S.F, T.C.S.F, I.P.S, and M.C designed experiments.N.S.F, T.C.S.F, I.P.S, J.B.A, V.C.O, D.B.A, J.W.B.D.J, C.C, A.F.P, and M.C performed experiments. N.S.F, T.C.S.F, I.P.S, D.I.S, J.B.A, V.C.O, D.B.A, A.F.P, R.P, W.A, and M.C analyzed data. N.SF, T.C.S.F, I.P.S, D.I.S, R.P, W.A, and M.C wrote and/or edited the manuscript. R.P, W.A, and M.C funded the project.

Declarations

Competing interests

R.P. and W.A. are founders and equity shareholders of PhageNova Bio. R.P. is the Chief Scientific Officer of and serves as a paid consultant for PhageNova Bio. R.P. and W.A. are founders and equity shareholders of and serve as paid consultants for MBrace Therapeutics. R.P. and W.A. have Sponsored Research Agreements (SRAs) in place with PhageNova Bio and with MBrace Therapeutics. These arrangements are managed in accordance with the established institutional conflict-of-interest policies of Rutgers, The State University of New Jersey. This particular study falls outside of the scope of these SRAs. The subject matter of this publication falls outside of SRAs of PhageNova Bio and MBrace Therapeutics. All the remaining authors declare no conflict of interest.

Additional information

Supplementary Information The online version contains supplementary material available at https://doi.org/10.1038/s41598-025-16761-4.

Correspondence and requests for materials should be addressed to W.A. or M.C.

Reprints and permissions information is available at www.nature.com/reprints.

Publisher's note Springer Nature remains neutral with regard to jurisdictional claims in published maps and institutional affiliations.